

Check for updates



Modeling of the Healing Process of Polycaprolactone-Interleaved Carbon Fiber-Reinforced Composites

Balázs Magyar¹ | Tibor Czigány¹.² | Dániel Török¹.³ | Gergő Zsolt Marton¹.⁴ | Fanni Balogh¹.⁴ | Gábor Szebényi¹.⁴ 🗓

¹Department of Polymer Engineering, Faculty of Mechanical Engineering, Budapest University of Technology and Economics, Budapest, Hungary | ²HUN-REN-BME Research Group for Composite Science and Technology, Budapest, Hungary | ³MTA-BME Lendület Lightweight Polymer Composites Research Group, Budapest, Hungary | ⁴MTA-BME Lendület Sustainable Polymers Research Group, Budapest, Hungary

Correspondence: Gábor Szebényi (szebenyi@pt.bme.hu)

Received: 8 February 2025 | Revised: 25 April 2025 | Accepted: 6 May 2025

Funding: This work was supported by Ministry of Culture and Innovation of Hungary, TKP2021-NVA; Magyar Tudományos Akadémia; Nemzeti Kutatási Fejlesztési és Innovációs Hivatal, KDP-2023.

Keywords: interface | multi-mechanism modeling | pseudo-ductile composite | self-healing

ABSTRACT

Thermoplastic interlayer provides an excellent opportunity to heal/repair inhomogeneities or damage in composites. By melting the thermoplastic interlayer, the damage can be filled, thereby increasing the service life of the composite part. In this paper, we analyzed the healing process of carbon fiber–reinforced epoxy matrix composites with a thermoplastic, structured interlayer (created by FFF 3D printing method) during ENF tests. We observed the effect of the concentration of the interlayer and the applied surface pressure on the properties of the healing process. The results show that increasing interlayer content can improve maximal healing efficiency from $96.6\% \pm 0.3\%$ ($25 \,\text{A/A}\%$) to $98.8\% \pm 0.3\%$ ($100 \,\text{A/A}\%$). While healing pressure does not affect the healing efficiency significantly, it can reduce the optimal healing time. In all cases, healing efficiency has an optimum, after which increased healing time leads to a decrease. To gain a deeper understanding of the process, we have adapted a control theory model, which helps in the selection of optimal process parameters for healing, which can be utilized for other thermoplastic interlayer-based healing methods.

1 | Introduction

In the past decade, the demand for carbon fiber-reinforced polymeric composites has rapidly grown due to their outstanding mechanical properties [1–3]. Composite systems, which consist of carbon fiber (CF) and epoxy resin (EP) tend to fail catastrophically, without any sign before the final failure happens. This catastrophic failure can be reduced by applying a thermoplastic interlayer, which increases the interlaminar fracture toughness. With thermoplastic interlayers, the CFRP systems tend to retain their structural integrity after reaching their maximal load capacity, with which damage also develops [4–8]. If only moderate damage is introduced, the created interlaminar damage can be

mended by filling with the molten interlayer material. By repairing/healing the damaged composites, the system's ecological footprint can be improved via reuse PEVuZE5vdGU [9, 10].

There are several methods to heal or repair damaged composites. We can separate the healing methods according to several properties [9, 10]. Based on the healing mechanism, a self-healing system can be intrinsic or extrinsic. Intrinsic systems provide the healing of the composite through molecular interactions by the matrix itself. Meanwhile, extrinsic systems work with pre-embedded external healing agents. Another possibility of the classification of self-healing mechanisms is the initiation of the healing process. Based on that,

This is an open access article under the terms of the Creative Commons Attribution-NonCommercial-NoDerivs License, which permits use and distribution in any medium, provided the original work is properly cited, the use is non-commercial and no modifications or adaptations are made.

© 2025 The Author(s). Polymer Composites published by Wiley Periodicals LLC on behalf of Society of Plastics Engineers.

Summary

- Healable composites were created with thermoplastic interlaminar patterns.
- Repeated ENF tests showed good healing performance.
- Effect of thermoplastic content, pressure, and time was investigated.
- Control theory model was created to optimize the process.

a system can be autonomous or assisted. A self-healing system is called autonomous when no external intervention is required to initiate the healing process. Autonomous methods include the microcapsule [11, 12], hollow fiber [13-15], and vascular methods [16–18]. The healing agent, which is mainly in liquid form, is incorporated in the matrix in the form of capsules (microcapsules), hollow fibers (mainly hollow glass fiber—HGF) or in a vascular system. The crack tear opens the elements containing the liquid healing agent; then, the liquid fills the resulting cracks or at least blunts crack tips. In the filled cracks, the liquid cross-links, completing the healing cycle. The advantage of the autonomous procedure is that, in most cases, the material of the healing agent is the same as the matrix material; thus, a strong connection can form between the phases. The disadvantage of the procedure is that the healing agent ages with time, and in most cases, healing can only be performed once [10, 14-16].

Healing methods that require external intervention are called assisted. In the case of these methods, usually a polymer (mostly thermoplastic) is embedded in the system. It can be distributed in the matrix or can be an interlayer. Mending occurs via an external energy stimulus (mostly heat), which causes reversible bonding. Hayes et al. [19, 20] used Poly(butyl acrylate) (PBA) as a healing agent, which was mixed into the resin before curing. Hayes et al. [19, 20] found that by increasing the temperature of mending, the healing efficiency of the impact-bent epoxy resin-PBA blends increased, which is also true for the composites they examined with the Mode I tests. In the case of composites, increasing the mass ratio of the PBA healing agent also increased the effectiveness of mending. Mending was performed at 130°C for 1 h without external pressure. Jony et al. [21], Luo et al. [22], Jiménez-Suárez et al. [23], Dorigato et al. [24], and Karger [25] used polycaprolactone (PCL) instead of PBA due to its relatively low melting temperature. They used the same method to incorporate the healing agent in the resin. They achieved similar results during the tests. In each study, the authors observed that the PCL filled the cracks due to its thermal expansion, which is different from that of the composite. An important difference is that the researchers used a different healing temperature (above melting temperature— T_m in all cases), different healing time, and a different pressure during the healing process. In addition to the dispersion of the healing agent in the resin, another possibility is the interlayer method, which can be used to improve interlaminar fracture toughness, thus improving several properties of the composite. With the help of the interlayer, crack propagation can be slowed, and so the composite system can absorb additional energy during failure. Wang et al. [26] used Ethylene Methacrylic Acid (EMAA) as an interlayer. By using EMAA films as an interlayer, the value of $G_{\rm Ic}$ improved significantly compared to the neat composites. After the initial $G_{\rm Ic}$ test, the specimens were mended at 150°C for 30 min. After mending was done, a second $G_{\rm Ic}$ test was carried out, where a healing efficiency of 42% was achieved. Furman et al. [27], Meure et al. [28], and Pingkarawat et al. [29] achieved similar results using EMAA films in various tests, but in all papers different mending parameters were used. The use of 3D printing techniques such as the fused filament fabrication (FFF) method to introduce designed thermoplastic interlayers [6] or create structured thermoplastic thermoset blends [24] is a widely researched hot topic in the field of self-healing, not only optimized pattern designs [30], but also biomimetic vascular systems can be created in the composite structure [31].

In the case of methods that require external intervention, the basic rule for mending temperature is that it should be above the melting temperature of the thermoplastic healing material. However, the researchers used a different temperature even for the same material; they used a different curing pressure and curing time. Also, the researchers did not examine the effect of the individual parameters on the effectiveness of the treatment. It is important to note that with both autonomous and assisted methods, only the damaged resin can be mended; fractured fibers cannot be healed.

The relevant literature shows that several studies were conducted related to the area of self-healing composites. However, these studies do not include any detailed investigation of the effects of different healing parameters, or any modeling of the healing process, which could lead to a deeper understanding of the mechanisms and key affecting factors leading to the healing of the composites. The aim of our research was to demonstrate the repeated healability of our interfacially engineered composites and to provide a method, which can be applied for other similar systems, which creates the possibility to optimize and model the healing process of self-healing systems incorporating thermoplastic healing agents.

We examined the effect of mending pressure and interlayer material content on the healing properties of CFRPs. For this, we used fused filament fabrication (FFF) to print the interlayer onto the surface of the fabrics. Afterwards, we carried out endnotched flexure (ENF) tests on the specimens. The ENF test setup was selected because it provides similar delamination propagation, as observed in bent structures with internal flaws. After the ENF tests, we mended the specimens with a hot press with various pressures and various mending times at a fixed temperature (above the melting temperature of the interlayer material— $T_{\rm m}$, under the glass transition temperature of the epoxy resin— $T_{\rm g}$) and then performed a second ENF test. Based on the results, we also modeled the process using control theory to gain a deeper insight into the dynamics of the process.

2 | Experimental

We used the IPOX ER 1010 (IPOX Chemicals Kft., Budapest, Hungary) DGEBA-based epoxy resin (EP) (epoxy equivalent weight: 188 g/eq, density: 1.1 g/cm³) as the matrix of the composite laminate with IPOX MH 3111 amine-based curing agent

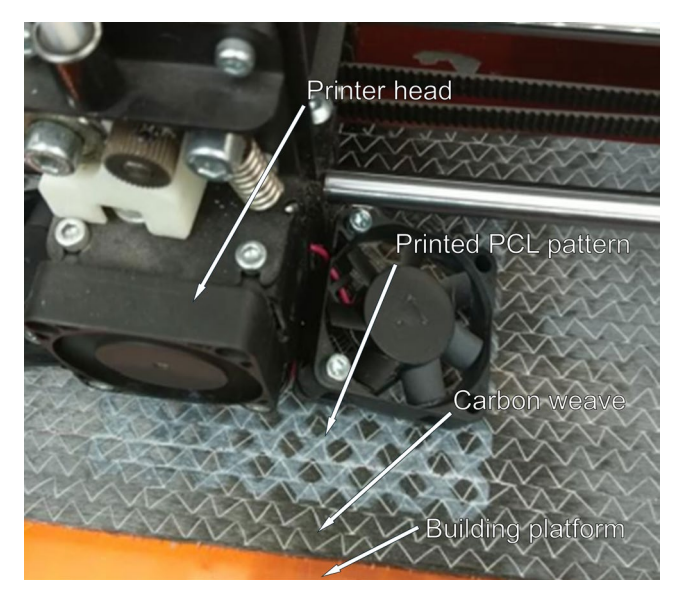


FIGURE 1 | Interlayer printing on the surface of CF.

TABLE 1 | FFF 3D printing parameters.

Printing temperature (°C)	180
Bed temperature (°C)	40
Layer height (MM)	0.2

(amine value: 460 mg KOH/g, density: 0.95 g/cm³). The mixing weight ratio was 100:75, according to the producer's recommendation. The EP was cured at 90°C. The resin system has a glass transition temperature (T_g) of 80°C. Fiber reinforcement was PX35FBUD0300 (Zoltek Zrt., Nyergesújfalu, Hungary) unidirectional carbon weave (309 g/m² surface weight), consisting of Panex35 50k rovings resulting in an average cured ply thickness of 0.37 mm. For the 3D printed interface, we selected eMorph175N05 (Shenzhen Esun Industrial Co. Ltd., Shenzhen, China) PCL filament. We chose PCL because it is soluble in the matrix, thus it does not create a new phase and it is easier to process than other thermoplastic additives. This is due to its lower melting temperature and because it is a biomaterial, so it is not harmful to the environment, unlike many high-performance additives. Filament diameter was 1.75 mm (density, $\rho = 1.16 \,\mathrm{g/cm^3}$, melting temperature, $T_{\mathrm{m}} = 60 \,\mathrm{^{\circ}C}$, print temperature: 180°C).

Fused filament fabrication (FFF) technology was used to manufacture the interfacial grid patterns (Figure 1). The main parameters of the 3D printing process are presented in Table 1. We used poly(ϵ -caprolactone) PCL as a surface modifier, which can be used to create a weakened bond between the matrix and the reinforcement. The basic geometry of the applied pattern is shown in Figure 1 with the dimensions in Table 2 (for three printed grids). We chose this based on our previous experimental results [32]. The increased surface fill rate was achieved by increasing the thickness of each zone. For FFF printing, we used a Craftbot Plus 3D printer.

Composite plates with $[0^{\circ}_{6}]$ layup sequence were manufactured. We printed on the middle CF fabric (3rd layer). In the case of

TABLE 2 | Interlayer grid dimensions.

	Surfac	ce filling (A/A	A%)
Length (mm)	25	50	100
x (line width)	1.0	2.2	_
y (line spacing)	7.0	5.8	_

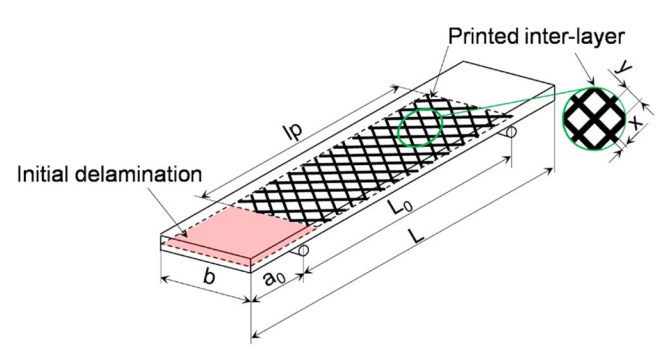


FIGURE 2 | Interlayered specimens for the ENF test.

the 100 A/A% surface filling grid, we printed a film covering the whole surface of the CF fabric. The laminates were manufactured via vacuum infusion.

We used flat glass molds for vacuum infusion with peel plies on both sides, which eased the removal of the PET film that covered the mold. Above the peel plies, we placed the resin guide net, which spread the resin evenly. A vacuum bag was built over the laminate to provide uniform pressure and high fiber content. A vacuum of 0.8 bar was applied for 3 h in a drying oven at 90°C. Under these conditions, PCL was only partly dissolved in the EP. The specimens were cut from the laminates with a Mutronic Diadisc diamond disc saw according to standard specifications. The dimensions of the specimens are shown in Figure 2.

The specimens contained the initial delamination between the same layers as the printed interlayer. In Figure 2, a_0 is the initial length of the delamination (45 mm), b is the width of the test specimen (25.4 mm), L_0 is the distance between the supports (120 mm), L is the length of the specimen (163 mm), and $l_{\rm p}$ is the length of the interlayer pattern (90 mm). Table 1 contains the dimensions of the printed interlayer (x—line width and y—line spacing definitions are presented in Figure 2).

3 | Results and Discussion

The initial damage was produced with ENF tests. The experimental setup is shown in Figure 3a. The ENF tests were performed until a 2.5% drop after maximum load. To calculate the interlaminar fracture toughness, we used Equation (1) [33]

$$G_{IIc} = \frac{9P_c^2 a_c^2 C_c}{2b(2L^3 + 3a_c^3)} \tag{1}$$

where $P_{\rm c}(N)$ is the maximum force, $a_{\rm c}$ (mm) is the critical length of the crack, and $C_{\rm c}$ is the critical compliance (mm/N). The critical



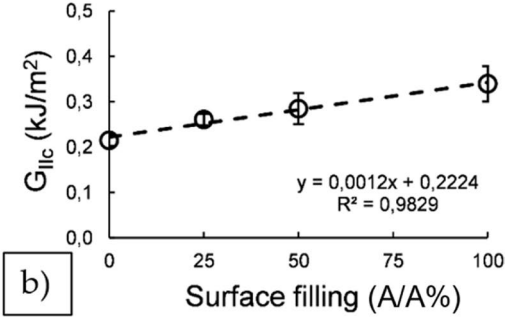


FIGURE 3 | (a) ENF test setup (1—ENF specimen on supports, 2—digital camera for crack tracking), (b) Initial interlaminar fracture toughness results.

crack length values were evaluated directly from the camera images; this method proved to be more precise compared to calculations because calculated $\rm a_c$ values typically underestimate the actual crack position. The initial interlaminar fracture toughness $(G_{\rm IIc})$ results are shown in Figure 3b. In the case of reference samples (specimens without the PCL interlayer) the laminates separated completely, and crack propagation was unstable. In contrast, in the 3D printed interlayered specimens, crack propagation was stable—after reaching maximal load capacity, the samples retained their structural integrity. Ten specimens were tested for each surface filling ratio. A Nikon 600D digital camera was used in video mode for constant crack front position tracking.

3.1 | The Effect of Applied Pressure on the Healing Process

After the initial damage via the ENF tests, the specimens were healed with a hot press with three different pressures. We used 1, 2, and 10 bar of surface pressure; the healing temperature was 65°C, which is above the melting temperature (T_m) of the PCL but below the glass transition temperature (T_g) of the EP, so structural integrity was not compromised. Before healing the specimens in the main experiments, the time required for the middle of the sample to reach the melting temperature of PCL was measured with thermocouples placed in the composite specimens as preliminary experiments. We have used a K-type thermocouple wire probe to measure the temperature between the middle plies of the composite. The data acquisition was performed with a Novus myPCLab unit with a 2Hz sampling rate. A total of 5 specimens were tested at 10 bar pressure. As seen in Figure 4, approximately 8s of dwell time in the heated platen press at 10 bar pressure is needed to reach the melting temperature of the added PCL. This is included in the dead times calculated in the modeling section.

Firstly, we checked if the sample without interlayer material showed any healing effect and proved that the epoxy used in the experiments had no healing capability. PCL interlayer concentration was fixed at 25 A/A%. With that, the thermoplastic can bleed, which can mend delaminated surfaces. The healing process was also carried out over different time intervals. In that way, we were able to evaluate the effect of pressure and time on the mending process. After the mending process, we tested the specimens again and compared the $G_{\rm IIc}$ values to the original (undamaged) $G_{\rm IIc}$ values. Using that, we calculated healing efficiency, as Equation (2) shows.

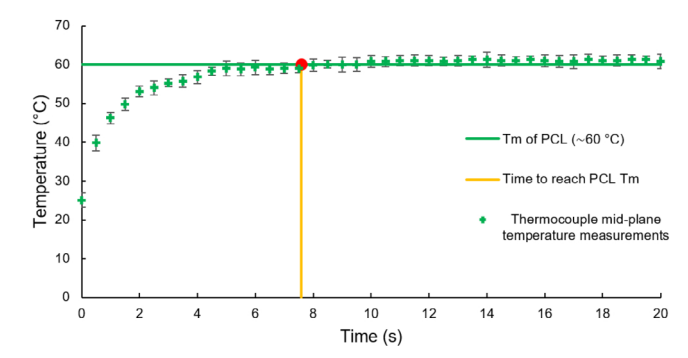


FIGURE 4 | Measured mid-plane temperature of the laminate during heat-up in platen press.

$$\eta = \frac{G_{IIc_{Healed}}}{G_{IIc_{Initial}}} \times 100 \tag{2}$$

where η is the healing efficiency (%), $G_{IIc\ initial}$ is the initial interlaminar fracture toughness (kJ/m 2), $G_{IIcHealed}$ is the interlaminar fracture toughness after healing (kJ/m²). Healing can be monitored if healing efficiency is plotted as a function of healing time. In the initial stage of healing, until the bleeding of the thermoplastic material started towards the cracks, healing efficiency hardly changes (a period of 10-15s in each case) (Figure 5). This is followed by a transition phase with different slopes for different treatment pressures. With higher pressure, the composite system reaches maximum healing efficiency faster. The reason for this is that as a result of higher pressure, the interface separations are filled more quickly with the thermoplastic material. The time derivative of healing shows that healing is faster when pressure is higher. The time required to reach maximum efficiency also decreases as pressure increases, and the state of equilibrium occurs sooner. With 10 bar, the healing efficiency vs. time curve decreases after reaching $\eta_{\rm max}$. This is more noticeable in the derivative of the curve, where negative values also appear with the decrease.

The decreasing trend can be explained by interlayer material melting and exiting towards the sides from the interface (Figure 6). Due to the high pressure, the thermoplastic material was able to leave the system more easily compared to low pressures. Weight loss starts with the onset of the deterioration of $G_{\rm IIc}$. The decreasing weight of a test specimen shows that 25% of the PCL material in the system melted and left the specimen, significantly reducing the thickness of the boundary layer. Thus, less thermoplastic material was present in the shear zone, less

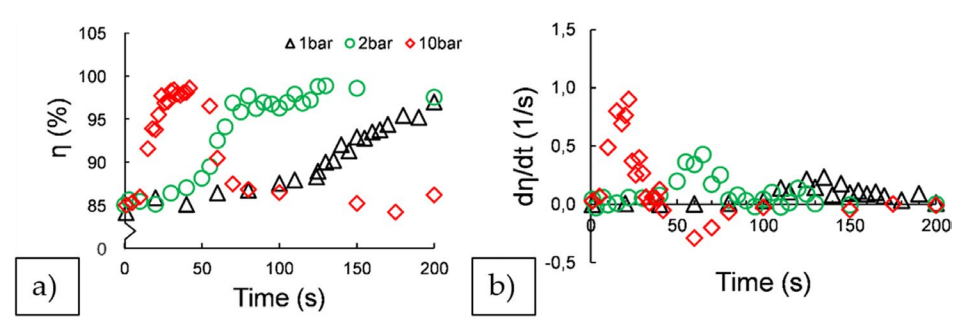


FIGURE 5 | (a) Effect of treatment pressure on the healing of composites in the case of interlaminar fracture toughness; (b) Time derivative of healing efficiency (PCL interlayer concentration was fixed at 25 A/A%).

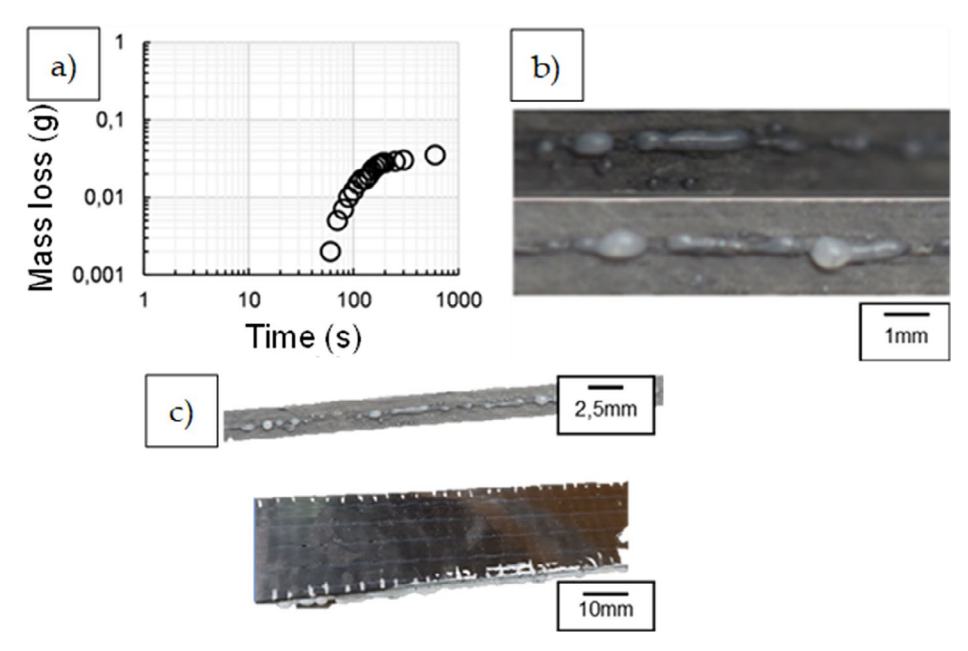


FIGURE 6 | Weight loss at a pressure of 10 bar; (a) relationship between time and mass loss on a logarithmic scale; (b) dissolving PCL from the side view in close-up shots; (c) melted interlayer material.

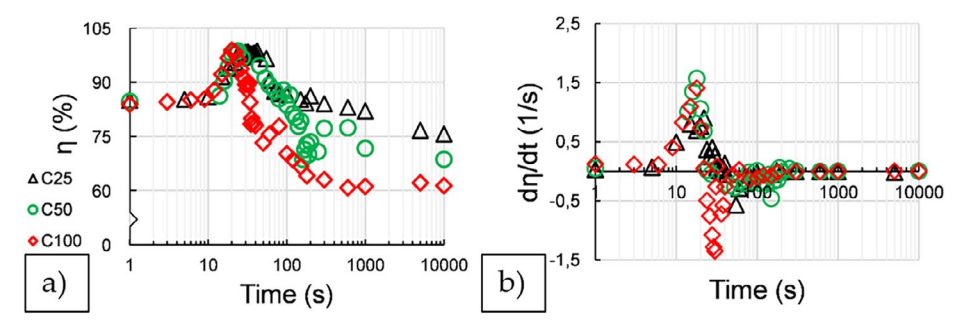


FIGURE 7 | Effect of concentration of the interlayer -25 (C25), 50 (C50) and 100 (C100) A/A%—on the interlayer fracture toughness of composites at a pressure of p = 10 bar; (a) healing efficiency; (b) time derivative of healing efficiency.

energy was required for crack propagation, and unstable crack propagation started earlier, even at a lower force.

3.2 | The Effect of Interlayer Content on the Healing Process

We carried out the tests at the surface concentration levels mentioned in the previous section (25, 50, and 100 A/A%) at

a fixed surface pressure of 10 bar (Figure 7). Each point in Figure 6 and onward represents a single measurement on a single specimen; we have chosen fine spacing of sampling points on the x-axis to show information not only about the trend but also the repeatability of the measurements. There was a difference between maximum healing efficiency levels with the different concentrations, which did not show any dependence on the applied pressure. Healing efficiency increased with increasing interlayer concentration. It was $96.6\% \pm 0.3\%$ for the

 $25\,\mathrm{A/A\%}$ samples, $97.4\%\pm0.2\%$ for the $50\,\mathrm{A/A\%}$ samples, and $98.8\%\pm0.3\%$ for the $100\,\mathrm{A/A\%}$ samples. The reason for this is that at a higher concentration level, more interlayer material is available for healing, so the material can fill the defects better. With increasing healing time, healing efficiency shows a saturation. With sufficient treatment time, the thermoplastic layer melts from the separated surfaces like previously. In this case, efficiency approaches the performance of the composites in which the delamination between the 3rd and 4th layers is present along its entire length. The time to reach saturation at a pressure of $10\,\mathrm{bar}$ is $1\,\mathrm{h}$.

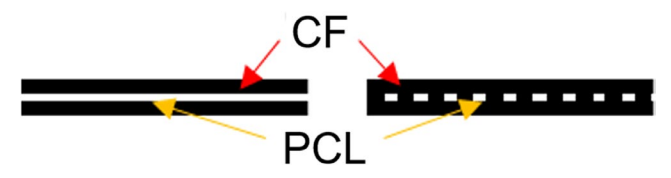


FIGURE 8 | Free surface of PCL interlayers at the edges of the specimens with different surface fillings.

The decrease in efficiency can be connected to the decrease in mass, just like the PCL loss experienced during the previous series of experiments. In the case of samples with a larger interlayer content, the speed of this decrease was faster and the PCL left the system sooner. This appeared due to the cutting of the specimens. In the case of samples with 100 A/A% surface fill, this provided a complete free surface in the middle layer for the melting of the thermoplastic layer. In the case of lower fill rates, the PCL was not exposed on the entire surface at the edge of the test specimens, so it left the system more slowly at the same pressure (Figure 8).

3.3 | Modeling the Healing Process

The healing process can be well approximated with the help of control theory models [34]. With the use of a model, the behavior of a system can be investigated regardless of concentration or healing pressure. For the model, it is necessary to determine the input signal $(X_{\rm in}(t))$ and the response of the system $(X_{\rm out}(t))$. Graphical definition of the two signals is essential to determine the appropriate transfer function (Figure 9a).

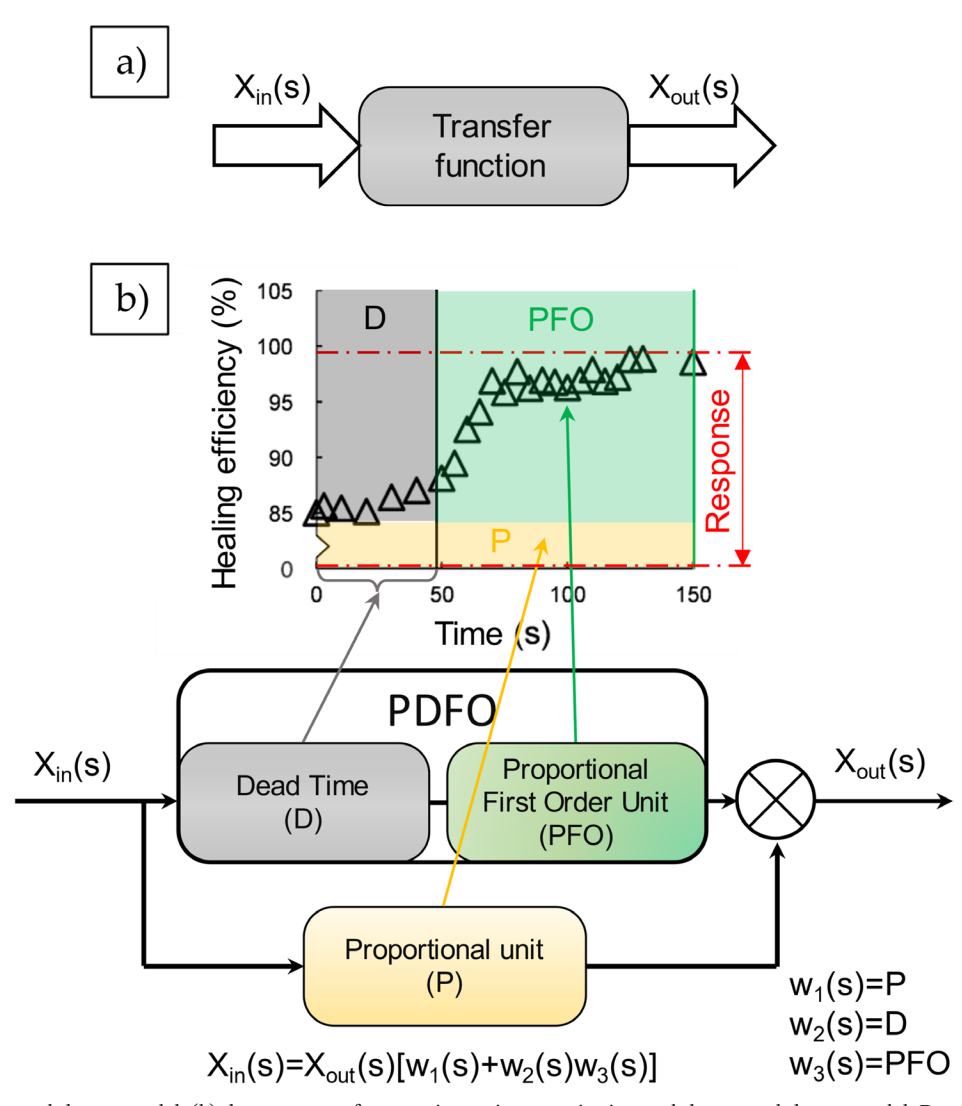


FIGURE 9 | (a) Control theory model, (b) the response of composites to jump excitation and the control theory model; D = dead time; P = proportional unit; PFO = proportional first order unit.

During the healing process, the excitation is pressure and heat. The response to this is that the interlayer material fills the cracks and separations over time. The nature of this transition can be determined based on the transient part of the response function. During repair, the efficiency of healing changes from an initial stable state to a new stable state; the efficiency of healing is the difference between the initial and the maximally achievable healing efficiency ($\Delta \eta = 15$, $G_{\rm IIc}$ ratio pairs of the actual and initial and maximally achievable values), which corresponds to a jump excitation. The response can be divided into several parts. A proportional response to the jump stimulus is generated during the first

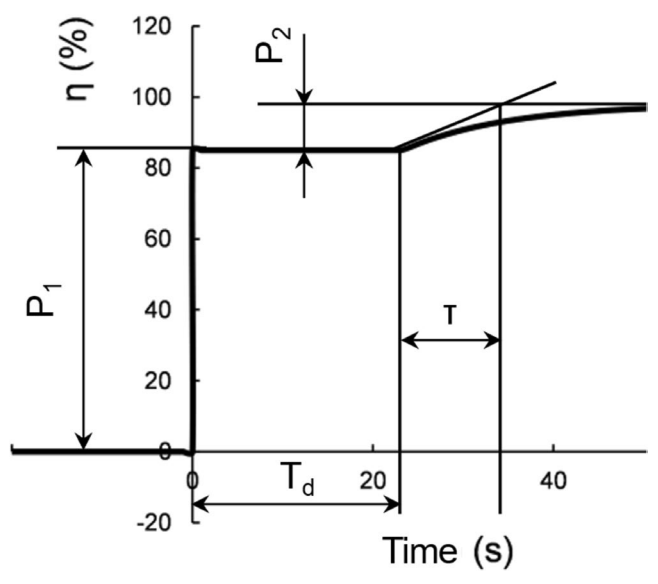


FIGURE 10 | Explanation of the parameters of the model used in the healing of partially damaged composites.

initial phase without delay. The reason for this is that the final failure did not occur during the first ENF tests, that is, the composites still maintained their integrity, so they were able to take up loads at the start of the next cycle, thus having an initial G_{He} value. This can be characterized with a proportional term (P₁). The value of P₁ is independent of the surface filling and pressure applied during the process. After this, a delay can be observed, that is, a further response to the jump excitation is not immediately generated. This can be defined with a dead time term (D) (due to the time required to bring the PCL to a viscous state). The transient that appears can be well approximated with a proportional first-order unit (PFO). This is because the equilibrium state needs time after the end of the dead time, that is, the stable state does not occur immediately. The parameters of the transfer function of the proportional first order are the system time constant (τ) and the proportionality factor (P2). The value of P2, which can be explained with the maximal achievable healing efficiency, varies with different concentrations, since none of the samples reached the theoretically achievable 100% cure, but by increasing surface filling, we were able to approach 100% better. Meanwhile, the value of τ influences the time required to reach the maximal achievable healing efficiency and depends on time and surface filling. The theoretical system model is shown in detail in Figure 9b.

The transfer function of the system can be described with a proportional unit connected in parallel with a PDFO (a dead time and a proportional first order unit connected in series). The length of dead time depends on pressures and surface filling (D) (Figure 8b). To determine the parameters, we used ordinary least squares. The fitted model can be defined with Equation (3),

$$X_{out_{(t)}} = P_{1_{(t)}} + P_{2_{(t-T_D)}} \left(1 - e^{-\frac{t-T_D}{\tau}} \right)$$
 (3)

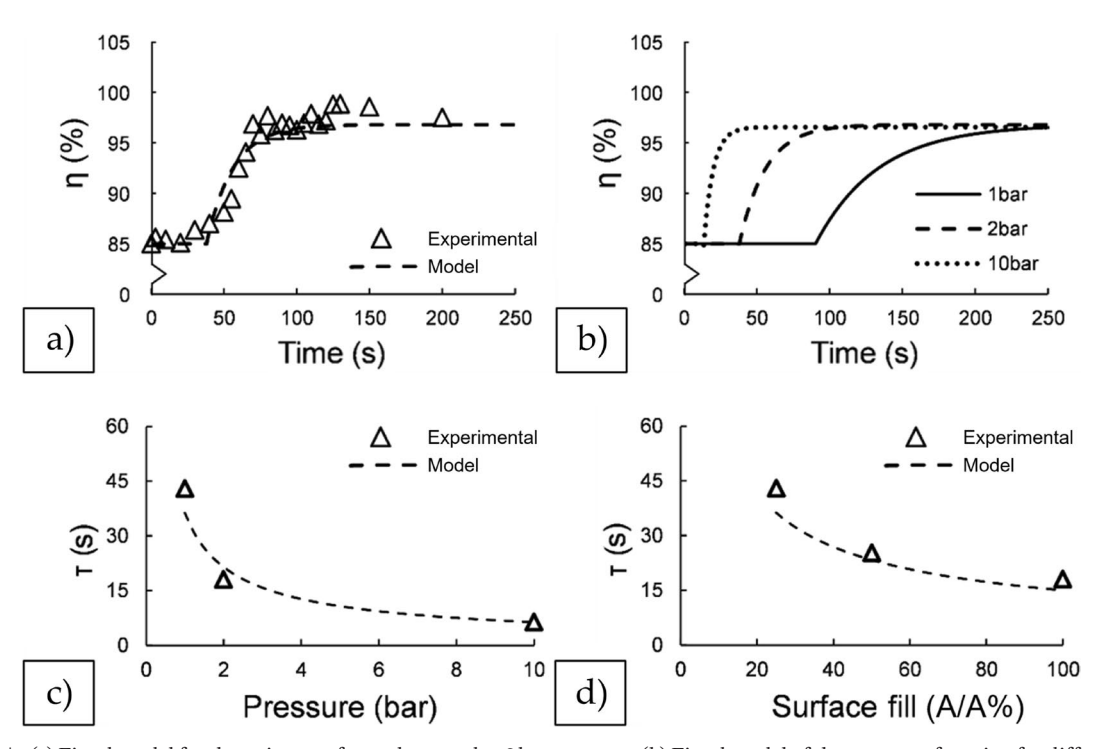


FIGURE 11 (a) Fitted model for the point set of samples cured at 2 bar pressure, (b) Fitted model of the response function for different pressures, (c) The dependence of the time constant on pressure during the healing process (C25); (d) The dependence of the time-constant on surface concentration during the healing process (p=1 bar).

where $X_{\mathrm{out}(i)}$ is the response (healing efficiency, η , %); P_1 is the remaining interlayer fracture toughness divided by the original value, the proportionality unit (%); P_2 is the proportionality unit (–); t is the healing time (s); the time constant τ (s) and dead time T_D (s). The parameters of the model are illustrated in Figure 10. At t=0, a proportional unit (P_1) immediately appears in the response to the jump excitation, which is followed by a dead time (D), after which the transient part appears, that is the proportional first order unit (with proportionality factor P_2 and time constant τ). With the help of the equation, the time required for the maximally achievable healing efficiency can be determined, but it is

not suitable for modeling the decrease caused by the thermoplastic material leaving the system. Modeling the latter requires that the equation is supplemented with an additional element connected in series with a dead time and single-storage proportional term.

Figure 11ab shows the fitted curves with different pressures. It shows that with higher pressure, the maximum heal ability of the system was reached sooner. However, at a pressure of 10 bar, the model can only be used within certain limits, up to the maximum healing efficiency. This is due to the fact that the decrease observed in the measurements, which is caused by the exiting

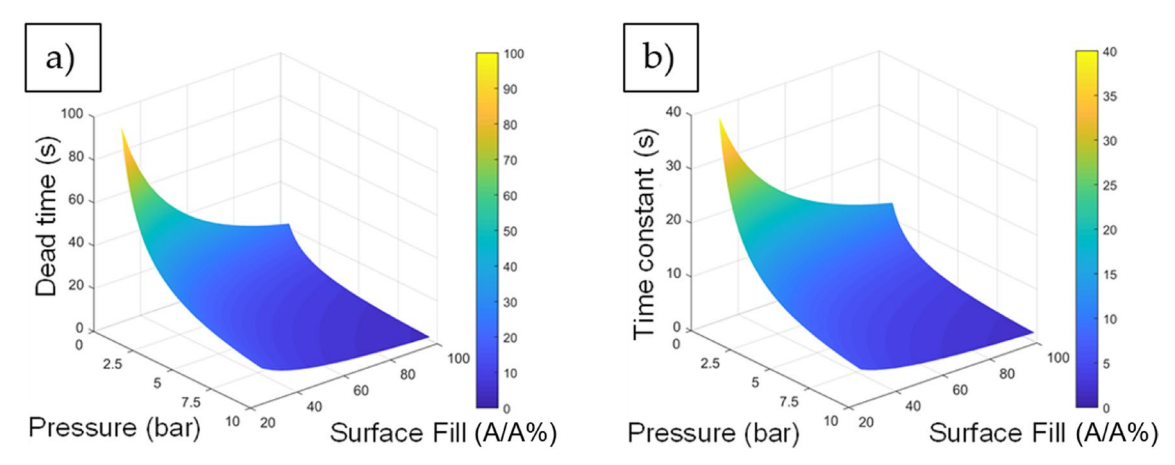


FIGURE 12 | The dependence of the (a) dead time and (b) time constant on pressure and concentration in the model of the healing of partially damaged composites.

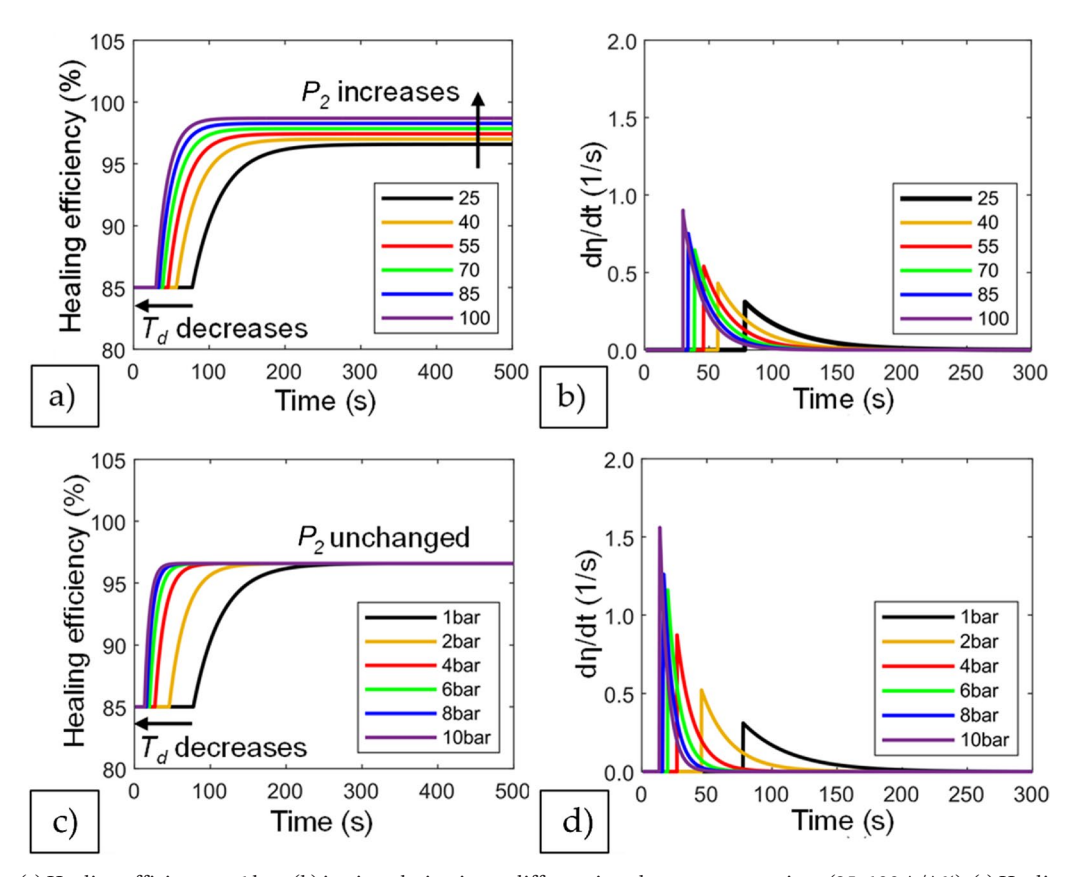


FIGURE 13 (a) Healing efficiency at 1 bar; (b) its time derivative at different interlayer concentrations (25–100 A/A%), (c) Healing efficiency with a fixed 25 A/A% at different pressures (1–10 bar); (d) its time derivative.

melted thermoplastic interlayer material, is not included in the model. However, the model is well suited for determining the optimal time for healing.

Based on our results, we also created a model for concentration and pressure based on the previous models. The time constant decreases significantly as the pressure increases, that is maximum efficiency is achieved in less time (Figure 11c,d). The pressure had a greater effect on this rate than the surface concentration of PCL. It indicates that surface fill has a smaller effect than pressure. Increasing pressure accelerates healing more.

A larger, comprehensive model can be formed from the two separate series of experiments, which can model both the pressure and concentration dependence of the system. Therefore, we performed the measurements at three different pressures, as well as with three different concentrations.

From the preliminary results, the parameters used during the fitting showed pressure- and concentration-dependent properties $(\tau, T_{\rm D})$. The reason for this is that during the process, the pressure accelerates reaction speed, so with higher pressures, the cracks are filled more quickly. Furthermore, concentration also affects the previous two factors in a similar way: at higher interlayer content, the necessary flow path is shorter, and the cracks are filled faster thanks to the excess material. In the case of the proportional term, only concentration dependence is observed. The reason for this is that the maximum achievable healing efficiency only depends on the PCL present in the system; the pressure can only influence the speed of the reaction.

We fitted a surface on $D_{\rm (c,p)}$ and of $\tau_{\rm (c,p)}$ as a function of pressure (1–10 bar) and surface fill (25–100 A/A%) with the MatLab program (Figure 12). The surfaces clearly show the dependence of dead time and time constant on these parameters. The behavior of the proportional member is linear.

At the surface pressure of 1 bar, interlayer content changes dead time and P_2 . Increasing the interlayer content decreases the time requirement for the transient part (decreases D), and also increases the maximal achievable healing efficiency (P_2). Furthermore, the derivative function shows that the reaction rate is also affected by concentration. By increasing the interlayer content, the recovery process speeds up and the derivative approaches 0 faster, that is the system can reach the maximum recovery for a given concentration level sooner. This is also true in the case of the dead time, which shows a continuous, exponential decrease on the curves describing the healing process (Figure 13a,b).

However, when pressure is changed, the proportional term does not change based on the statement discussed above. The dead time term and τ also show parameter dependence here, just like in the case of surface fill. Similarly, to the curves of increasing surface fill, with increasing pressure, dead time continuously decreases, which is also true for the time constant (Figure 13c,d).

4 | Conclusion

We have developed a new qualification method, which is suitable for characterizing the healing process of composite samples

of carbon fiber-reinforced epoxy resin composites with an interlayer of polycaprolactone damaged with end-notched flexure tests. The measurement procedure is based on observing the change in critical interlaminar fracture toughness; thereby, the change in the healing process and its effectiveness can be followed.

The results show that healing efficiency increases with increasing interlayer concentration from $96.6\% \pm 0.3\%$ (25 A/A%) to $98.8\% \pm 0.3\%$ (100 A/A%). Meanwhile, healing pressure does not have any significant effect on the healing efficiency, although the time necessary for reaching maximal healing efficiency can be reduced by increasing healing pressure. In each case, after exceeding the optimal healing time, healing efficiency decreases, which can be explained by the bleeding of PCL thermoplastic interlayer material.

We showed that the healing process can be described with a control theory model. The control theory model consists of a proportional unit connected in parallel with the dead time and proportional first-order unit connected in series (Figure 9). With the help of the equation, the time required for the maximal achievable healing efficiency can be determined, but it is not suitable for modeling the decrease caused by the melting of the thermoplastic material.

Author Contributions

The authors take full responsibility for this article.

Acknowledgments

We would like to sincerely thank the late Prof. Dr. h.c. mult. József Karger-Kocsis for his support and valuable comments, which serve as a solid foundation of our research. The research has been supported by the NRDI Office (OTKA FK 142540). Gábor Szebényi acknowledges the financial support received through the János Bolyai Scholarship of the Hungarian Academy of Sciences and ÚNKP-23-5-BME-415 New National Excellence Program. Project no. 2022-2.1.1-NL-2022-00012 National Laboratory for Cooperative Technologies has been implemented with the support provided by the Ministry of Culture and Innovation of Hungary from the National Research, Development, and Innovation Fund, financed under the National Laboratories funding scheme. Project no. TKP-6-6/ PALY-2021 has been implemented with the support provided by the Ministry of Culture and Innovation of Hungary from the National Research, Development and Innovation Fund, financed under the TKP2021-NVA funding scheme. Project no. KDP-IKT-2023-900-I1-00000957/0000003 has been implemented with the support provided by the Ministry of Culture and Innovation of Hungary from the National Research, Development and Innovation Fund, financed under the KDP-2023 funding scheme. The project supported by the Doctoral Excellence Fellowship Programme (DCEP) is funded by the National Research Development and Innovation Fund of the Ministry of Culture and Innovation and the Budapest University of Technology and Economics.

Conflicts of Interest

The authors declare no conflicts of interest.

Data Availability Statement

The data that support the findings of this study are available from the corresponding author upon reasonable request.

References

- 1. P. Csvila and T. Czigány, "Multifunctional Energy Storage Polymer Composites: The Role of Nanoparticles in the Performance of Structural Supercapacitors," *Express Polymer Letters* 18 (2024): 1023–1038, https://doi.org/10.3144/expresspolymlett.2024.78.
- 2. B. Messaoud and M. N. Amrane, "Vibration Analysis of Damaged Viscoelastic Composite Sandwich Plate," *Periodica Polytechnica, Mechanical Engineering* 68, no. 2 (2024): 85–96, https://doi.org/10.3311/PPme.19466.
- 3. A. Alipour, R. Lin, and K. Jayaraman, "Enhancement of Performance in Flax/Epoxy Composites by Developing Interfacial Adhesion Using Graphene Oxide," *Express Polymer Letters* 17 (2023): 471–486, https://doi.org/10.3144/expresspolymlett.2023.35.
- 4. N. Sela, O. Ishai, and L. Banks-Sills, "The Effect of Adhesive Thickness on Interlaminar Fracture Toughness of Interleaved Cfrp Specimens," *Composites* 20, no. 3 (1989): 257–264, https://doi.org/10.1016/0010-4361(89)90341-8.
- 5. S. García Rodríguez, J. Costa, K. Rankin, R. Boardman, V. Singery, and J. Mayugo, "Interleaving Light Veils to Minimise the Trade-Off Between Mode-I Interlaminar Fracture Toughness and In-Plane Properties," *Composites Part A: Applied Science and Manufacturing* 128 (2019): 105659, https://doi.org/10.1016/j.compositesa.2019. 105659.
- 6. B. Beylergil, "Interlaminar Fracture and Crack-Healing Capability of Carbon Fiber/Epoxy Composites Toughened With 3D-Printed Poly-ε-Caprolactone Grid Structures," *Journal of Applied Polymer Science* 139, no. 17 (2022): 52038, https://doi.org/10.1002/app.52038.
- 7. M. T. M. Alshrif, Y. Peng, Z. Yang, et al., "Interlaminar Toughening of Carbon Fiber/Epoxy Composites via Interleaving co-Polyamide (Co-PA) Veils," *Polymer Composites* 45, no. 16 (2024): 14549–14565, https://doi.org/10.1002/pc.28781.
- 8. D. K. Too, S. Kumar, and Y.-H. Kim, "Fracture Toughness and Failure Behavior of CF/Epoxy Composites Interleaved With Melt-Infused PET, PEI, and PEEK Film," *Polymer Composites* 45, no. 13 (2024): 12307–12324, https://doi.org/10.1002/pc.28637.
- 9. J. A. Syrett, C. R. Becer, and D. M. Haddleton, "Self-Healing and Self-Mendable Polymers," *Polymer Chemistry* 1, no. 7 (2010): 978–987, https://doi.org/10.1039/C0PY00104J.
- 10. A. Cohades, C. Branfoot, S. Rae, I. Bond, and V. Michaud, "Progress in Self-Healing Fiber-Reinforced Polymer Composites," *Advanced Materials Interfaces* 5, no. 17 (2018): 1800177, https://doi.org/10.1002/admi. 201800177.
- 11. E. N. Brown, M. R. Kessler, N. R. Sottos, and S. R. White, "In Situ Poly(Urea-Formaldehyde) Microencapsulation of Dicyclopentadiene," *Journal of Microencapsulation* 20, no. 6 (2003): 719–730, https://doi.org/10.3109/02652040309178083.
- 12. J. D. Rule, E. N. Brown, N. R. Sottos, S. R. White, and J. S. Moore, "Wax-Protected Catalyst Microspheres for Efficient Self-Healing Materials," *Advanced Materials* 17, no. 2 (2005): 205–208, https://doi.org/10.1002/adma.200400607.
- 13. R. S. Trask, G. J. Williams, and I. P. Bond, "Bioinspired Self-Healing of Advanced Composite Structures Using Hollow Glass Fibres," *Journal of the Royal Society Interface* 4, no. 13 (2007): 363–371, https://doi.org/10.1098/rsif.2006.0194.
- 14. G. Williams, R. Trask, and I. Bond, "A Self-Healing Carbon Fibre Reinforced Polymer for Aerospace Applications," *Composites Part A: Applied Science and Manufacturing* 38, no. 6 (2007): 1525–1532, https://doi.org/10.1016/j.compositesa.2007.01.013.
- 15. S. Kling and T. Czigány, "Damage Detection and Self-Repair in Hollow Glass Fiber Fabric-Reinforced Epoxy Composites via Fiber Filling," *Composites Science and Technology* 99 (2014): 82–88, https://doi.org/10.1016/j.compscitech.2014.05.020.

- 16. C. J. Hansen, W. Wu, K. S. Toohey, N. R. Sottos, S. R. White, and J. A. Lewis, "Self-Healing Materials With Interpenetrating Microvascular Networks," *Advanced Materials* 21, no. 41 (2009): 4143–4147, https://doi.org/10.1002/adma.200900588.
- 17. K. S. Toohey, C. J. Hansen, J. A. Lewis, S. R. White, and N. R. Sottos, "Delivery of Two-Part Self-Healing Chemistry via Microvascular Networks," *Advanced Functional Materials* 19, no. 9 (2009): 1399–1405, https://doi.org/10.1002/adfm.200801824.
- 18. J. F. Patrick, K. R. Hart, B. P. Krull, et al., "Continuous Self-Healing Life Cycle in Vascularized Structural Composites," *Advanced Materials* 26, no. 25 (2014): 4302–4308, https://doi.org/10.1002/adma.201400248.
- 19. S. A. Hayes, F. R. Jones, K. Marshiya, and W. Zhang, "A Self-Healing Thermosetting Composite Material," *Composites Part A: Applied Science and Manufacturing* 38, no. 4 (2007): 1116–1120, https://doi.org/10.1016/j.compositesa.2006.06.008.
- 20. S. A. Hayes, W. Zhang, M. Branthwaite, and F. R. Jones, "Self-Healing of Damage in Fibre-Reinforced Polymer-Matrix Composites," *Journal of the Royal Society Interface* 4, no. 13 (2007): 381–387, https://doi.org/10.1098/rsif.2006.0209.
- 21. B. Jony, M. Thapa, S. B. Mulani, and S. Roy, "Repeatable Self-Healing of Thermosetting Fiber Reinforced Polymer Composites With Thermoplastic Healant," *Smart Materials and Structures* 28, no. 2 (2019): 025037, https://doi.org/10.1088/1361-665X/aaf833.
- 22. X. Luo, R. Ou, D. E. Eberly, A. Singhal, W. Viratyaporn, and P. T. Mather, "A Thermoplastic/Thermoset Blend Exhibiting Thermal Mending and Reversible Adhesion," *ACS Applied Materials and Interfaces* 1, no. 3 (2009): 612–620, https://doi.org/10.1021/am8001605.
- 23. A. Jiménez-Suárez, G. Del Rosario, X. X. Sánchez-Romate, and S. G. Prolongo, "Influence of Morphology on the Healing Mechanism of PCL/Epoxy Blends," *Materials* 13, no. 8 (2020): 1941, https://doi.org/10.3390/ma13081941.
- 24. A. Dorigato, D. Rigotti, and A. Pegoretti, "Novel Poly(Caprolactone)/ Epoxy Blends by Additive Manufacturing," *Materials* 13, no. 4 (2020): 819, https://doi.org/10.3390/ma13040819.
- 25. J. Karger-Kocsis, "Self-Healing Properties of Epoxy Resins With Poly(ε-Caprolactone) Healing Agent," *Polymer Bulletin* 73, no. 11 (2016): 3081–3093, https://doi.org/10.1007/s00289-016-1642-2.
- 26. C. H. Wang, K. Sidhu, T. Yang, J. Zhang, and R. Shanks, "Interlayer Self-Healing and Toughening of Carbon Fibre/Epoxy Composites Using Copolymer Films," *Composites Part A: Applied Science and Manufacturing* 43, no. 3 (2012): 512–518, https://doi.org/10.1016/j.compositesa. 2011.11.020.
- 27. S. Meure, R. J. Varley, D. Y. Wu, S. Mayo, K. Nairn, and S. Furman, "Confirmation of the Healing Mechanism in a Mendable EMAA–Epoxy Resin," *European Polymer Journal* 48, no. 3 (2012): 524–531, https://doi.org/10.1016/j.eurpolymj.2011.11.021.
- 28. S. Meure, D. Y. Wu, and S. Furman, "Polyethylene-Co-Methacrylic Acid Healing Agents for Mendable Epoxy Resins," *Acta Materialia* 57, no. 14 (2009): 4312–4320, https://doi.org/10.1016/j.actamat.2009.05.032.
- 29. K. Pingkarawat, C. H. Wang, R. J. Varley, and A. P. Mouritz, "Mechanical Properties of Mendable Composites Containing Self-Healing Thermoplastic Agents," *Composites Part A: Applied Science and Manufacturing* 65 (2014): 10–18, https://doi.org/10.1016/j.compositesa.2014.05.015.
- 30. J. S. Turicek, A. D. Snyder, K. B. Nakshatrala, and J. F. Patrick, "Topological Effects of 3D-Printed Copolymer Interlayers on Toughening and In Situ Self-Healing in Laminated Fiber-Composites," *Composites Science and Technology* 240 (2023): 110073, https://doi.org/10.1016/j.compscitech.2023.110073.
- 31. Z. Wan, Y. Xu, Y. Zhang, S. He, and B. Šavija, "Mechanical Properties and Healing Efficiency of 3D-Printed ABS Vascular Based Self-Healing Cementitious Composite: Experiments and Modelling," *Engineering*

Fracture Mechanics 267 (2022): 108471, https://doi.org/10.1016/j.engfracmech.2022.108471.

- 32. B. Magyar, T. Czigany, and G. Szebényi, "Metal-Alike Polymer Composites: The Effect of Inter-Layer Content on the Pseudo-Ductile Behaviour of Carbon Fibre/Epoxy Resin Materials," *Composites Science and Technology* 215 (2021): 109002, https://doi.org/10.1016/j.compscitech.2021.109002.
- 33. M. A. Azmah Hanim, D. Brabazon, and M. S. J. Hashmi, "8—Cracks, Microcracks, and Fracture Toughness of Polymer Composites: Formation, Testing Method, Nondestructive Detection, and Modifications," in *Failure Analysis in Biocomposites, Fibre-Reinforced Composites and Hybrid Composites*, ed. M. Jawaid, M. Thariq, and N. Saba (Woodhead Publishing, 2019), 157–180.
- 34. S. A. Marshall, *Introduction to Control Theory* (Macmillan Education UK, 1978).